THE JOURNAL OF BIOLOGICAL CHEMISTRY VOL. 288, NO. 18, pp. 12852–12865, May 3, 2013
© 2013 by The American Society for Biochemistry and Molecular Biology, Inc. Published in the U.S.A.

Nuclear Factor κB Mediates Suppression of Canonical Transient Receptor Potential 6 Expression by Reactive Oxygen Species and Protein Kinase C in Kidney Cells*

Received for publication, December 11, 2012, and in revised form, March 21, 2013 Published, JBC Papers in Press, March 22, 2013, DOI 10.1074/jbc.M112.410357

Yanxia Wang[‡], Min Ding[‡], Sarika Chaudhari[‡], Yanfeng Ding[‡], Joseph Yuan[‡], Dorota Stankowska[§], Shaoqing He[§], Raghu Krishnamoorthy[§], Joseph T. Cunningham[‡], and Rong Ma[‡1]

From the [‡]Department of Integrative Physiology and Cardiovascular Research Institute and the [§]Department of Cell Biology, University of North Texas Health Science Center, Fort Worth, Texas 76107

Background: TRPC6 expression in glomerular cells is suppressed by ROS through a PKC mechanism.
Results: Activation and inhibition of NF-κB could mimic and inhibit the ROS/PKC effect on TRPC6 expression, respectively.
Conclusion: NF-κB mediates the inhibitory effect of ROS/PKC on TRPC6 expression in mesangial cells.
Significance: This study delineated a molecular mechanism for regulation of TRPC6 at the transcriptional level.

This study was carried out to explore the molecular mechanism for down-regulation of TRPC6 expression in the reactive oxygen species (ROS)/PKC signaling in kidney cells. In cultured human mesangial cells, H_2O_2 and TNF-α inhibited TRPC6 mRNA expression in a time-dependent manner. Inhibition of NF-κB reversed both H_2O_2- and phorbol 12-myristate 13-acetate (PMA)-induced decrease in TRPC6 protein expression. Activation of NF-κB by knocking down IκBα using siRNA could mimic the suppressive effect of ROS/PKC on TRPC6. a Ca^{2+} imaging study showed that activation and inhibition of NF-κB significantly decreased and increased the TRPC6-mediated Ca^{2+} entry, respectively. Further experiments showed that PMA, but not its inactive analog 4α-phorbol 12, 13-didecanoate (4α-PDD), caused phosphorylation of IκBα and stimulated the nuclear translocation of NF-κB p50 and p65 subunits. The PMA-dependent IκBα phosphorylation was significantly inhibited by Gö6976. Electrophoretic mobility shift assay revealed that PMA stimulated DNA binding activity of NF-κB. Furthermore, specific knockdown of p65, but not p50, prevented an H_2O_2 inhibitory effect on TRPC6 protein expression, suggesting p65 as a predominant NF-κB subunit repressing *TRPC6*. In agreement with a major role of p65, chromatin immunoprecipitation assays showed that PMA treatment induced p65 binding to the *TRPC6* promoter. Moreover, PMA treatment increased the association of p65 with histone deacetylase (HDAC) and decreased histone acetylation at the *TRPC6* promoter. Consistently, knockdown of HDAC2 by siRNA or inhibition of HDAC with trichostatin A prevented a H_2O_2-induced decrease in TRPC6 mRNA and protein expressions, respectively. Taken together, our findings imply an important role of NF-κB in a negative regulation of *TRPC6* expression at the gene transcription level in kidney cells.

TRPC6 belongs to the TRPC[2] family, which is composed of seven members, named TRPC1–7 (1). All TRPCs are Ca^{2+}-conductive non-selective cation channels and are globally expressed with implications to a variety of cellular functions from gene expression to cell proliferation (2). Over the past few years, we and others have demonstrated that TRPC6 was involved in vascular tone (3), diabetic kidney disease (4, 5), idiopathic pulmonary hypertension (6, 7), focal segmental glomerulosclerosis (8, 9), and cardiac hypertrophy (10). A multifunctional TRPC6 channel is tightly gated/regulated by multifactorial pathways to maintain cellular homeostasis. In the long history of exploring how TRPC6 channel is controlled, tremendous efforts have been made to uncover the acute mechanisms for regulation of the channels. These include membrane receptor activation (11), intracellular Ca^{2+} store depletion (12), stretch, membrane lipids (13), ROS (3, 14, 15), protein kinases (16–18), and trafficking (14, 19). However, how TRPC6 channel is regulated at the transcriptional level remains unknown. Our recent studies demonstrated that ROS acutely (in minutes) activated TRPC6 channels in vascular smooth muscle cells (3) but suppressed TRPC6 channel expression with prolonged exposure (in hours) in renal glomerular MCs (5). Because many diseases such as diabetes and hypertension are characterized with oxidative stress with chronic progression (20–23), identification of mechanisms for chronic regulation of TRPC6 channels by ROS has clear clinical significance.

Glomerular MCs sit between glomerular capillary loops and maintain the structural architecture of the capillary networks. These cells play important roles in mesangial matrix homeostasis, regulation of glomerular filtration rate, and phagocytosis of apoptotic cells in glomerulus (24–26). MC dysfunction is closely associated with several glomerular diseases, such as diabetic nephropathy (27–29). Previous studies from our group

* This work was supported, in whole or in part, by National Institutes of Health Grant 5 RO1 DK079968-01A2 (NIDDK; to R. M.). This work was also supported by American Heart Association South Central Affiliate Grant-in-aid 11GRNT7560013 (to R. M.).

[1] To whom correspondence should be addressed: 3500 Camp Bowie Blvd., Dept. of Integrative Physiology, University of North Texas Health Science Center, Fort Worth, TX 76107. Tel.: 817-735-2516; Fax: 817-735-5084; E-mail: rong.ma@unthsc.edu.

[2] The abbreviations used are: TRPC, transient receptor potential; NF-κB, nuclear factor κB; ROS, reactive oxygen species; PMA, phorbol 12-myristate 13-acetate; 4α-PDD, 4α-phorbol 12, 13-didecanoate; HDAC, histone deacetylase; MC, mesangial cell; IDT, integrated density value; CNAP1, chromosome condensation-related SMC-associated protein 1; MTT, 3-[4,5-dimethylthiazol-2-yl]-2,5 diphenyl tetrazolium bromide.

demonstrated that TRPC6 was expressed in MCs (30) and regulated MC function. The abundance of TRPC6 protein was significantly reduced in human MCs with chronic treatment with ROS via a PKC mechanism (5). However, the detailed molecular mechanism downstream of ROS/PKC is unknown. In the present study we showed evidence that NF-κB was the mediator linking ROS/PKC to TRPC6 expression by repressing *TRPC6* gene transcription.

EXPERIMENTAL PROCEDURES

MC Culture and Transient Transfection—Human MCs belong to Clonetics™ renal MC system and were purchased from Lonza (Walkersville, MD). MCs were cultured in low glucose (5.6 mM) DMEM medium (Invitrogen) supplemented with 25 mM HEPES, 4 mM glutamine, 1.0 mM sodium pyruvate, 0.1 mM nonessential amino acids, 100 units/ml penicillin, 100 μg/ml streptomycin, and 20% FBS. Cells were growth-arrested with 0.5% FBS medium during treatments. Only subpassages less than nine generations were used this study.

All siRNA oligonucleotides, including scramble control sequences, were transiently transfected into MCs using DharmaFECT 2 transfection reagent (Thermo Scientific, Rockford, IL) following the protocols provided by the manufacturer and described in Ref. 14. Seventy-two hours after transfection, cells were either harvested for Western blot or used for a fura-2 study.

3-[4,5-Dimethylthiazol-2-yl]-2,5 Diphenyl Tetrazolium Bromide (MTT) Assay—The MTT assay was conducted to evaluate cell viability in the presence of H_2O_2. MCs were plated in one 96-well with $\sim 30 \times 10^3$/100 μl/well 1 day before the assay. Cells were treated with 10 μl of the 12 mM MTT (EMD Millipore, Billerica, MA) stock solution and were incubated at 37 °C for 4 h. The medium was then removed, and 50 μl of DMSO were added to each well. After incubation at 37 °C for 10 min, absorbance at 540 nm with a reference wavelength of 570 nm was measured.

Quantitative Real Time RT-PCR—The total RNA was isolated from cultured human MCs using a PerfectPure RNA cultured cell kit (5 Prime, Inc., Hamburg, Germany) following the manufacturer's protocol. Human TRPC6 primers (forward, GCCAATGAGCATCTGGAAAT; reverse, TGGAGTCACATCATGGGAGA) and β-actin primers (forward, ACTGTGTGGATTACATGGGCCAGA; reverse, AGGATTGCCTCCACAATCCGTACA) were synthesized by IDT (Coralville, Iowa). iScript cDNA synthesis kit (Bio-Rad) was used for RT reactions with 1.0 μg of total RNA in a final volume of 20 μl following the manufacturer's reaction protocol. Real time PCR used 0.2 μg of RT product, 100 nM primer, and was performed using iQ SYBR Green supermix (Bio-Rad) in a final volume of 20 μl. The PCR mix was denatured at 95 °C for 10 min followed by 45 cycles of melting at 95 °C for 15 s, annealing at 57 °C for 10 s, and elongation at 72 °C for 15 s. After amplification, a melting curve analysis from 65 to 95 °C with a heating rate of 0.02 °C/s with a continuous fluorescence acquisition was made. The assay was run on a C1000™ Thermal Cycler (Bio-Rad). The average C_t (threshold cycle) of fluorescence units was used to analyze the mRNA levels. The TRPC6 mRNA levels were normalized by β-actin mRNA levels. Quantification was calculated as follows: mRNA levels $= 2^{\Delta(\Delta Ct)}$, where $\Delta C_t = C_{t,TRPC6} - Ct_{,actin}$·$\Delta(\Delta C_t) = \Delta C_{t,T} - \Delta C_{t,0}$, where $\Delta C_{t,T}$ represents ΔC_t at different time points of H_2O_2 treatment, and $\Delta C_{t,0}$ represents ΔC_t without H_2O_2 treatment.

Preparation of Nuclear Extracts—Preparation of nuclear extracts from human MCs was performed using Thermo Scientific NE-PER Nuclear and Cytoplasmic Extraction kit (Thermo Scientific) following the manufacturer's protocol. The extracts were stored at −80 °C until use.

Western Blots—As described in our previous publication (5). Briefly, the whole cell lysates or nuclear extracts were fractionated by 10% SDS-PAGE, transferred to PVDF membranes, and probed with primary TRPC6, actin, phospho-IκBα (Ser-32), IκBα, p50, p65, and lamin A/C antibodies. Bound antibodies were visualized with Super Signal West Femto (all proteins except actin) or Pico (for actin) Luminol/Enhancer Solution (Thermo Scientific). The specific protein bands were visualized and captured using an AlphaEase FC Imaging System (Alpha Innotech, San Leandro, CA). The IDT of each band was measured by drawing a rectangle outlining the band using AlphaEase FC software with auto background subtraction. If a protein had double bands, a total IDT by summation of each band IDT was used, The expression levels of TRPC6, phospho-IκBα, and IκBα proteins were quantified by normalization of the IDTs of those protein bands to that of actin bands on the same blot. In Fig. 10, the expression levels of nuclear p50 and p65 proteins were normalized to lamin A/C.

Coimmunoprecipitation of Nuclear Proteins—Nuclear extracts (50 μg) from human MCs with various treatments (Fig. 11*A*) were incubated with 2 μg of p65 primary antibody to pull down the nuclear p65 protein following the protocol described in our previous publication (31). The precipitated proteins were resolved by regular Western blot and probed with a HDAC2 antibody. A nuclear protein, lamin A/C, from 10 μg of the corresponding nuclear extracts was used as an input.

Fluorescent Immunocytochemistry—Human MCs were plated on 22 × 22–1 mm glass coverslips. Cells with or without pretreatments as indicated in Fig. 7*C* were fixed with 4% paraformaldehyde for 15 min at room temperature. After being washed with PBS, the cells were then incubated with ice-cold acetone at −20 °C for 10 min. After 30 min of incubation with blocking buffer, the cells were incubated with either p50 or p65 primary antibody at 1:400 and 1:100, respectively, in PBS plus 10% donkey serum and 0.2% Triton X-100 at 4 °C overnight. After three washes with PBS, the cells were then incubated with goat anti-rabbit secondary antibodies conjugated with Alexa Fluor 568 (for p50) or with Alexa Fluor 488 (for p65) (Invitrogen) at a concentration of 1:500 for 1 h at room temperature. DAPI (Invitrogen) was used for staining nuclei. For a fluorescent staining control, equal amounts of rabbit IgG were used instead of the primary antibodies. Localization of NF-κB subunits were visualized by Leica Confocal Laser Scanning microscope (Zeiss LSM 510).

EMSA—EMSA was performed using a double-stranded oligonucleotide containing a consensus binding sequence for κB (5′-AGTTGAG<u>GGGACTTTCC</u>CAGGC-3′), in which the underlined sequence represents the κB binding consensus. The nucleotides were end-labeled with biotin using a biotin 3′ end

DNA labeling kit (Thermo Scientific). Nuclear extracts (5 μg of protein) were incubated in 1× binding buffer containing 2.5% glycerol, 50 ng/μl poly(dI-dC), 5 mM $MgCl_2$, 0.05% Nonidet P-40, and 4 pmol of biotin-labeled oligonucleotide in a total volume of 20 μl at room temperature for 20 min. The reaction mixture was then subjected to electrophoresis in a 6% polyacrylamide gel using 0.5 × Tris borate EDTA as the running buffer. For competition studies, nuclear extracts were incubated with a 50-fold molar excess of unlabeled oligonucleotide. After transfer to nylon membrane at 100 V for 30 min at 4 °C, the membrane was then cross-linked for 60 s in a UV cross-linker. The binding complexes were then developed using Chemiluminescent Nucleic Acid Detection Module from Thermo Scientific following the manufacturer's protocol.

ChIP Assay—After MCs were treated as indicated in Figs. 10 and 11*B*, cells were cross-linked by 1% formaldehyde for 10 min at room temperature. Glycine was then added at a final concentration of 0.125 M to neutralize formaldehyde. After two washes with PBS, cells were scraped and collected by centrifugation (750 × *g*). Cells were then resuspended in lysis buffer 1 (50 mM HEPES-KOH, pH 7.5, 140 mM NaCl 1 mM EDTA, 10% glycerol, 0.5 Nonidet P-40, 0.25% Triton X-100, and a proteinase inhibitor mixture) and incubated at 4 °C for 10 min. Nuclei were then isolated by centrifugation (1350 × *g*) and lysed in lysis buffer 2 (10 mM Tris-HCl, pH 8.0, 200 mM NaCl, 1 mM EDTA, 0.5 mM EGTA, and a protease inhibitor mixture). The pelleted chromatin was then resuspended in lysis buffer 3 (10 mM Tris-HCl, pH 8.0, 100 mM NaCl, 1 mM EDTA, 0.5 mM EGTA, 0.1% sodium deoxycholate, 0.5% *N*-lauroylsarcosine, and proteinase inhibitor). After sonication, a 1/10 volume of 10% Triton X-100 was added to the lysates followed by centrifugation at 20,000 × *g* at 4 °C for 10 min, and the supernatants were incubated with 2 μg of p65 antibody (Abcam, Cambridge, MA) or a control rabbit IgG (Cell Signaling Technology, Danvers, MA) overnight at 4 °C. After immunoprecipitation, the samples were incubated with 25 μl of Magnetic A/G beads (Thermo Scientific) for 2 h at room temperature, and the immune complexes were collected by Magnetic Stand and washed 4 times with radioimmune precipitation assay buffer (10 mM Tris-HCl, 0.25 M LiCl, 0.5% Nonidet P-40, and 0.5% sodium deoxycholate, pH 7.5) followed by 2 washes with Tris-EDTA buffer with 50 mM NaCl. Then 50 μl of 10% Chelex 100 were added to the washed bead pellets, and the samples were boiled for 10 min at 100 °C. The pellets were then incubated with RNase for 1 h and proteinase K for 30 min at 55 °C. The supernatants were collected after maximum speed centrifugation (20,000 × *g*) at room temperature and subjected to quantitative real-time PCR or regular PCR. A volume of 2 μl of immunoprecipitated DNA was analyzed by real-time PCR (25 μl reaction mixture) using the iQ SYBR Green Supermix (Bio-Rad). Specificity of the assay was tested by amplification of *GAPDH* gene not bound by NF-κB (negative control). Primers flanking the κB sites at the *TRPC6* promoter were 5′-CGC TAC CAC CAG CGG CCC-3′ and 5′-GCC CAC TGG CCC GGG GAA AA-3′, designed to amplify a 143-bp product. The primers flanking the κB sites at the *IκBα* promoter were 5′-GAA GGA CTT TCC AGC CAC TC-3′ and 5′-GGA ATT TCC AAG CCA GTC AG-3′, designed to amplify a 163-bp product. The primers for *GAPDH* were 5′-ATG GTT GCC ACT GGG GAT CT-3′ and 5′-TGC CAA AGC CTA GGG GAA GA-3′, designed to amplify a 174-bp product.

A volume of 2 μl of the immunoprecipitated chromatin from the cells with different treatments was analyzed by real-time PCR. The PCR was performed in duplicate using iQ SYBR Green Supermix reagents (Bio-Rad). Real time-PCR conditions used were 95 °C for 3 min and 40 cycles with 95 °C for 15 s, 55 °C for 30 s, and 72 °C for 30 s. Melting curves were measured in the PCR machine between 60 and 95 °C with a resolution of 0.5 °C.

Fluorescence Measurement of $[Ca^{2+}]_i$—Measurements of $[Ca^{2+}]_i$ in MCs using fura-2 were performed using dual excitation wavelength fluorescence microscopy. MCs grown on a coverslip (22 × 22 mm) were loaded with fura-2 by incubation for 50 min at room temperature in the dark in physiological saline solution containing 2 μM acetoxymethyl ester of fura-2 (fura-2/AM), 0.09 g/dl DMSO, and 0.018 g/dl Pluronic F-127 (Invitrogen) followed by washing 3 times. The cells were then incubated with fura-2-free physiological saline solution for an additional 20 min. The coverslip was then placed in a perfusion chamber (Warner, Model RC-2OH) mounted on the stage of a Nikon Diaphot inverted microscope. Fura-2 fluorescence was monitored by a ratio technique (excitation at 340 and 380 nm, emission at 510 nm) using NIS Elements AR™ software (Nikon Instruments Inc., Melville, NY) at room temperature. $[Ca^{2+}]_i$ was calculated using the software following the manufacturer's instructions. Calibrations were performed *in vivo* at the end of each experiment, and conditions of high $[Ca^{2+}]_i$ were achieved by the addition of 5 μM ionomycin, whereas conditions of low $[Ca^{2+}]_i$ were obtained by the addition of 5 mM EGTA.

Materials and Reagents—The siRNA oligonucleotides against human IκBα, p50, and p65 were designed and synthesized by Cell Signaling Technology. The control scramble siRNA (Nontargeting siRNA #1, D-001810-01-20) was purchased from Thermo Scientific. InSolution™ NF-κB activation inhibitor and helenalin were purchased from Calbiochem. Rabbit anti-IκBα and rabbit anti-phospho-IκBα (Ser32) antibodies were purchased from Cell Signaling Technology. Mouse anti-p50, rabbit anti-p65, and rabbit anti-Lamin A/C antibodies were purchased from Biolegend (San Diego, CA). The anti-p65 antibody used in ChIP experiments was purchased from Abcam. The rabbit anti-acetyl histone H3 antibody was purchased from Millipore. DAPI was purchased from Invitrogen. Protease Inhibitor Mixture tablets were obtained from Roche Applied Science. All other primary antibodies and chemicals were purchased from Sigma.

Statistical Analysis—Data are reported as the means ± S.E. One-way analysis of variance plus Student-Newman-Keuls post hoc analysis and Student's unpaired *t* test were used to analyze the differences among multiple groups and between two groups, respectively. $p < 0.05$ was considered statistically significant. Statistical analysis was performed using SigmaStat (Jandel Scientific, San Rafael, CA).

RESULTS

TRPC6 mRNA Level Was Decreased by H_2O_2 in MCs—We have previously demonstrated that H_2O_2 reduced the abundance of TRPC6 protein in human MCs through a PKC mech-

anism (5). To determine whether the H_2O_2 effect was at a transcriptional or translational level, we conducted quantitative real-time RT-PCR using samples from human MCs either without H_2O_2 treatment or with H_2O_2 treatment for various time periods. As shown in Fig. 1, H_2O_2 induced a time-dependent decrease in TRPC6 mRNA steady-state levels, and a significant decrease was observed after 2 h of treatment (Fig. 1). These data suggest that H_2O_2 inhibited TRPC6 expression by suppression of *TRPC6* gene.

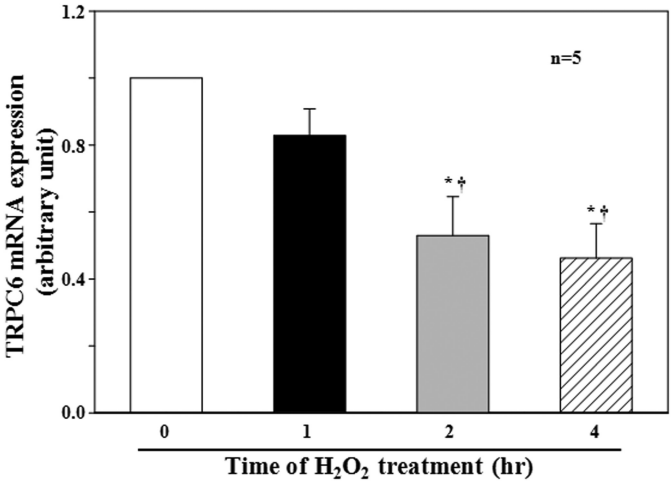

FIGURE 1. **Effect of H_2O_2 on TRPC6 mRNA expression in human MCs.** Cells were without (time 0) or with H_2O_2 treatment at 200 μM for 1, 2, and 4 h in FBS-free medium. The mRNA level of TRPC6 was determined by real-time RT-PCR and normalized by β-actin mRNA levels. * denotes $p < 0.05$, compared with time 0, and † denotes $p < 0.05$, compared with 1 h. *n* indicates the number of independent experiments.

NF-κB-mediated H_2O_2 and PKC-induced Reduction of TRPC6 Protein Expression in MCs—NF-κB is a well known transcription factor downstream of both ROS and PKC (32–35). To determine if this was also the case in suppression of TRPC6 expression by the cascade of H_2O_2/PKC, we assessed TRPC6 protein expression in MCs treated with H_2O_2 or phorbol 12-myristate 13-acetate (PMA) in the presence and absence of NF-κB inhibition. As shown in Fig. 2, *A* and *C*, H_2O_2 at 200 μM for 6 h significantly decreased TRPC6 protein abundance, and this inhibitory effect was completely prevented by NF-κB activation inhibitor (10 μM) but not by its vehicle (DMSO). H_2O_2 treatment did not affect MC viability assessed by MTT assay (data not shown). Consistent with our previous study (5), PMA, but not its inactive analog 4α-PDD significantly decreased TRPC6 expression (Fig. 2, *Ba* and *Da*). The PMA effect was also abolished by NF-κB inhibition with NF-κB activation inhibitor (10 μM) and Helenalin (1 μM) (Fig. 2, *Bb* and

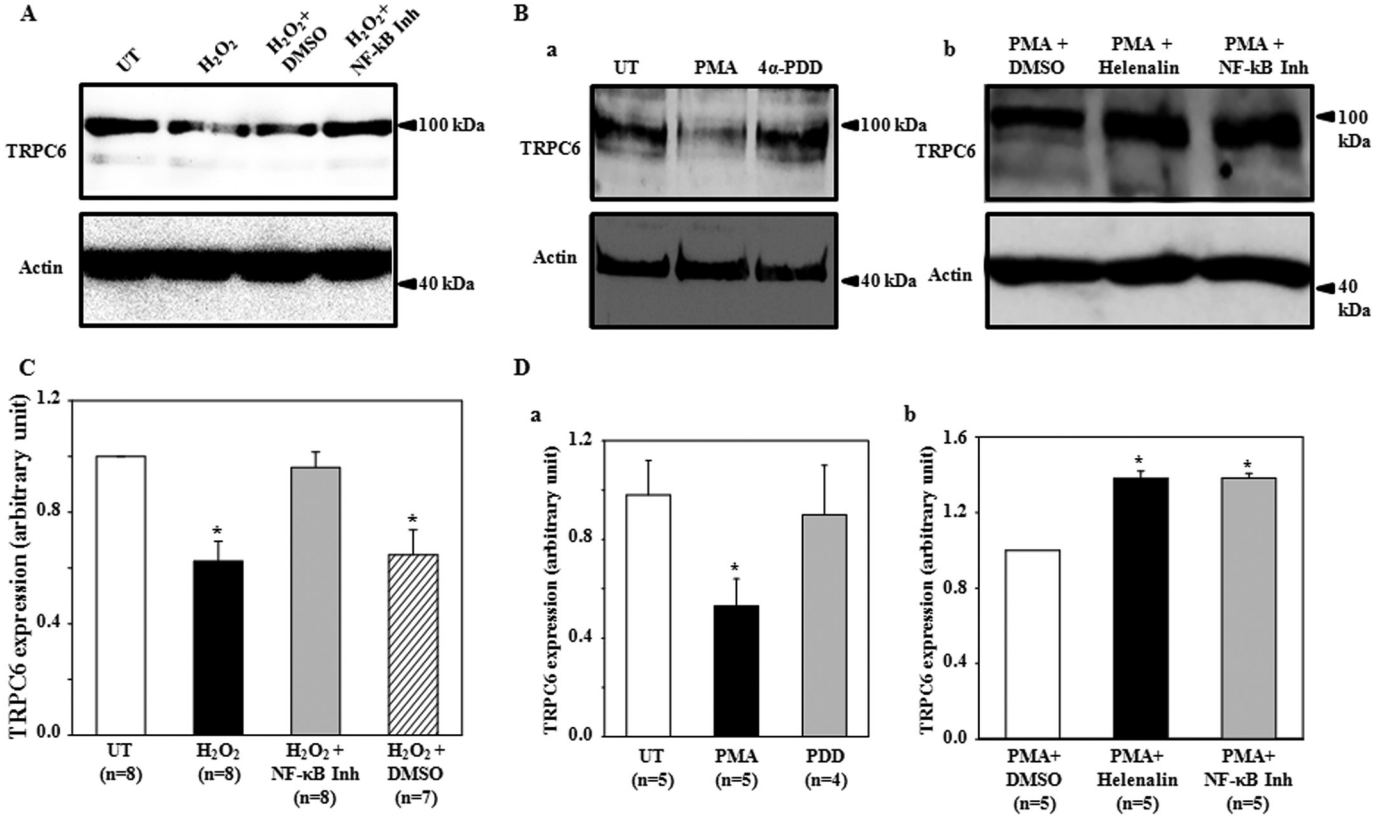

FIGURE 2. **A Western blot shows the effects of NF-κB inhibition of H_2O_2- and PMA-induced decrease in TRPC6 protein expression in human MCs.** *A*, shown is TRPC6 protein expression in MCs with (H_2O_2) or without (*UT*) exposure to 200 μM H_2O_2 for 6 h in the presence or absence of InSolution™ NF-κB activation inhibitor (*NF-κB Inh*) or DMSO. DMSO served as a vehicle control for InSolution™ NF-κB activation inhibitor. Both InSolution™ NF-κB activation inhibitor (10 μM) and DMSO were applied to MCs 30 min before H_2O_2 treatment and stayed in medium throughout H_2O_2 treatment. *B*, in *a*, TRPC6 protein expression is shown in MCs with PMA or 4α-PDD treatment (1 μM for 3 h) or without treatment (*UT*). In *b*, TRPC6 protein expression is shown in PMA-treated MCs with helenalin (1 μM) or InSolution™ NF-κB (NF-κB Inh, 10 μM) or DMSO pretreatment (30 min before and throughout PMA treatment). In *A* and *B*, actin was used as an internal loading control. *C* and *D*, quantifications of TRPC6 protein expression from the experiments are shown in *A* and *B*, respectively. TRPC6 expression was semiquantified by normalizing TRPC6 band optical density to its corresponding actin band optical density, and the ratio in group *UT* (for *C* and *Da*) or in group *PMA+DMSO* (for *Db*) was taken as 1. * denotes $p < 0.05$, compared with UT (*C* and *Da*) or PMA+DMSO (*Db*). *n* indicates the number of independent experiments.

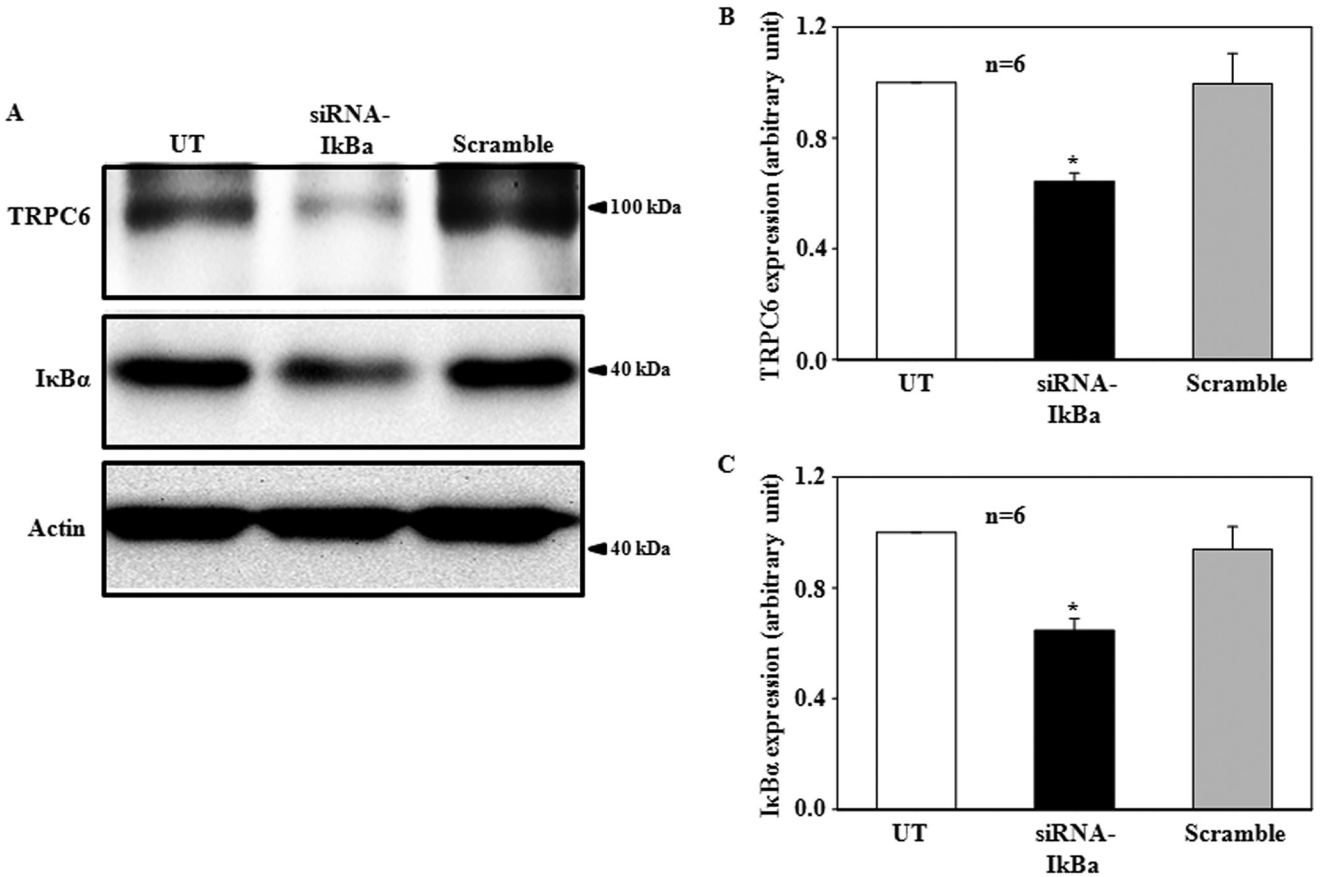

FIGURE 3. **A Western blot shows the effect of knockdown of IκBα on TRPC6 protein expression in human MCs.** *A*, a representative experiment shows TRPC6 protein expression in MCs without transfection (*UT*) or transfected with siRNA against human IκBα (*siRNA-IκBα*) or with scramble sequence (*Scramble*). Actin was used as a loading control. *B* and *C*, summary data show TRPC6 (*B*) and IκBα (*C*) expression levels (normalized to actin) in the groups indicated in *A*. * represents a significant difference as compared with both UT and Scramble. *n* indicates the number of independent experiments.

Db). These results suggest NF-κB is a downstream molecule of ROS and PKC in the suppression of TRPC6 protein expression.

Activation of NF-κB Decreased TRPC6 Protein Expression in MCs—The major form of NF-κB is a heterodimer of the p50 and p65/RelA subunits that are localized to the cytoplasm as a latent form (36). In unstimulated cells, the p50 and p65/RelA complex is retained in the cytoplasm by association with the inhibitor of NF-κB, IκB (36). Thus, removal of the inhibitory IκB is required for NF-κB activation. To determine if NF-κB negatively regulated TRPC6 expression, we activated endogenous NF-κB in human MCs by knocking down the prototypical IκB, IκBα, using siRNA. Compared with the MCs without transfection and with transfection with scramble siRNA, the IκBα expression level in the MCs transfected with siRNA against human IκBα reduced significantly (Fig. 3). Corresponding to this decrease, the abundance of TRPC6 protein decreased significantly (Fig. 3). These data suggest that direct activation of NF-κB could mimic ROS and PKC effect on TRPC6 expression and, thus, support the idea that NF-κB is a component in the TRPC6 regulation cascade.

NF-κB Activity Influenced TRPC6-mediated Ca^{2+} Entry in MCs—We next carried out Ca^{2+} imaging study to examine the functional consequence of NF-κB effect on TRPC6 protein expression. Hyperforin has been used by us and others to specifically activate TRPC6 channels (3, 37, 38). In the present study we used hyperforin to stimulate Ca^{2+} entry via TRPC6 channels in MCs with and without activation or inhibition of NF-κB. Ca^{2+} entry response was evaluated using a classical Ca^{2+} omission-addition protocol (3). In the first line of experiments, TRPC6-mediated Ca^{2+} influx was assessed in MCs with and without knocking down IκBα. In untransfected cells, re-addition of Ca^{2+} itself elevated the intracellular Ca^{2+} concentration ($[Ca^{2+}]_i$) by 66.9 ± 6.4 nM. Hyperforin (10 μM) significantly increased the Ca^{2+} response to 197.2 ± 48.1 nM (Fig. 4*B*). However, activation of NF-κB by siRNA against IκBα abolished the hyperforin-enhanced Ca^{2+} influx, but scramble transfection did not (Fig. 4, *A* and *B*). In the second line of experiments, we examined if inactivation of NF-κB could augment TRPC6-mediated Ca^{2+} entry. In MCs growth-arrested for 6 h, hyperforin treatment evoked a rise of $[Ca^{2+}]_i$ by 103.5 ± 20.9 nM upon Ca^{2+} re-addition into the bath. With H_2O_2 treatment (200 μM for 6 h in FBS free medium), the hyperforin response was significantly attenuated. Pretreatment of the cells with NF-κB activation inhibitor reversed the H_2O_2 inhibitory effect (Fig. 4, *C* and *D*). Furthermore, NF-κB inhibitor itself also significantly increased basal Ca^{2+} entry (without hyperforin stimulation) upon Ca^{2+} re-addition (Fig. 4*E*). These fura-2 data provided functional evidence for a negative regulation of TRPC6 channels by NF-κB.

PMA Phosphorylated IκBα in Human MCs—If NF-κB mediated a ROS/PKC-induced decrease in TRPC6 expression, then activation of PKC is expected to activate NF-κB. It has been

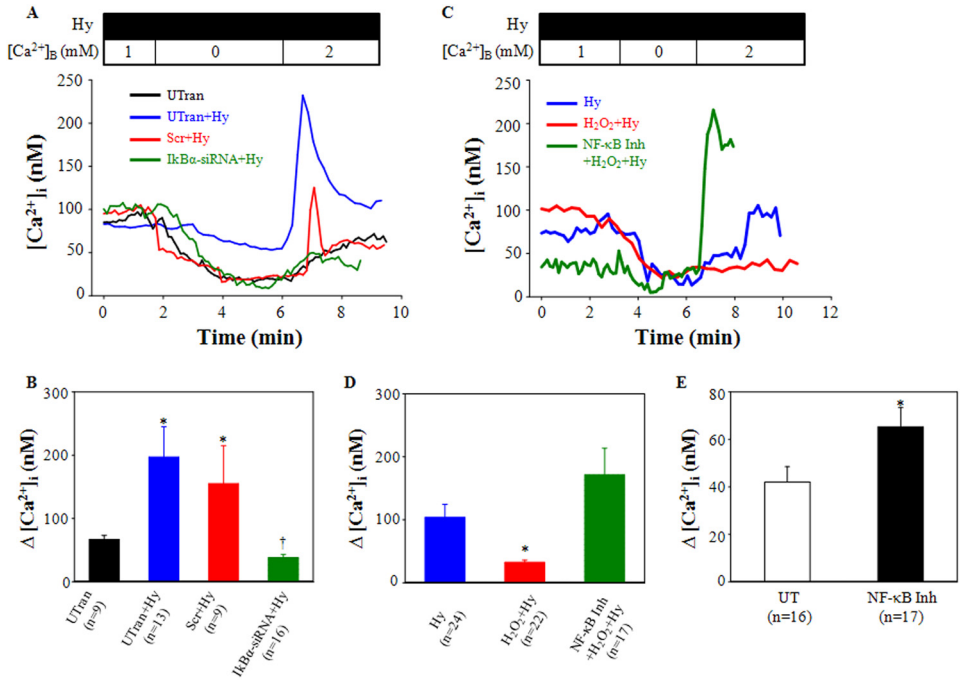

FIGURE 4. **Effect of NF-κB activity on TRPC6-mediated Ca^{2+} entry in human MCs.** *A*, representative traces show $[Ca^{2+}]_i$ in untransfected (*UTran*) MCs with or without hyperforin (*Hy*) treatment or in the scramble siRNA (*Scr+Hy*)- or IκBα siRNA (*siRNA+Hy*)-transfected MCs treated with hyperforin. *B*, shown are summarized Ca^{2+} responses from the experiments presented in *A*. *, $p < 0.01$, compared with untransfected. †, $p < 0.05$, compared with all other groups. *C*, shown are representative $[Ca^{2+}]_i$ traces in MCs treated with hyperforin (*Hy*) with or without prior incubation with H_2O_2 (200 μM for 6 h) in the presence or absence of InSolution™ NF-κB activation inhibitor (*NF-κB Inh*, 10 μM). Cells with or without H_2O_2 treatment were growth-arrested for 6 h before hyperforin stimulation. In both *A* and *C*, hyperforin (10 μM) was applied 30 min before experiments and was included in the bathing solution throughout the experiments. $[Ca^{2+}]_B$ indicates the Ca^{2+} concentration in bathing solution. All the traces were smoothed using the 2D smooth function of SigmaPlot program. *D*, summarized Ca^{2+} responses from experiments are presented in *C*. *, $p < 0.01$, compared with both Hy and H_2O_2+Hy. *E*, Ca^{2+} entry response in MCs without (*UT*) and with InSolution™ NF-κB activation inhibitor (*NF-κB Inh*) (10 μM) in 0.5% FBS medium for 6 h. *, $p < 0.05$, compared with UT. In *B*, *D*, and *E*, $\Delta[Ca^{2+}]_i$ was the difference in $[Ca^{2+}]_i$ before and after the addition of 2 mM Ca^{2+} to the bath. The *numbers inside the parentheses* represent the number of cells analyzed.

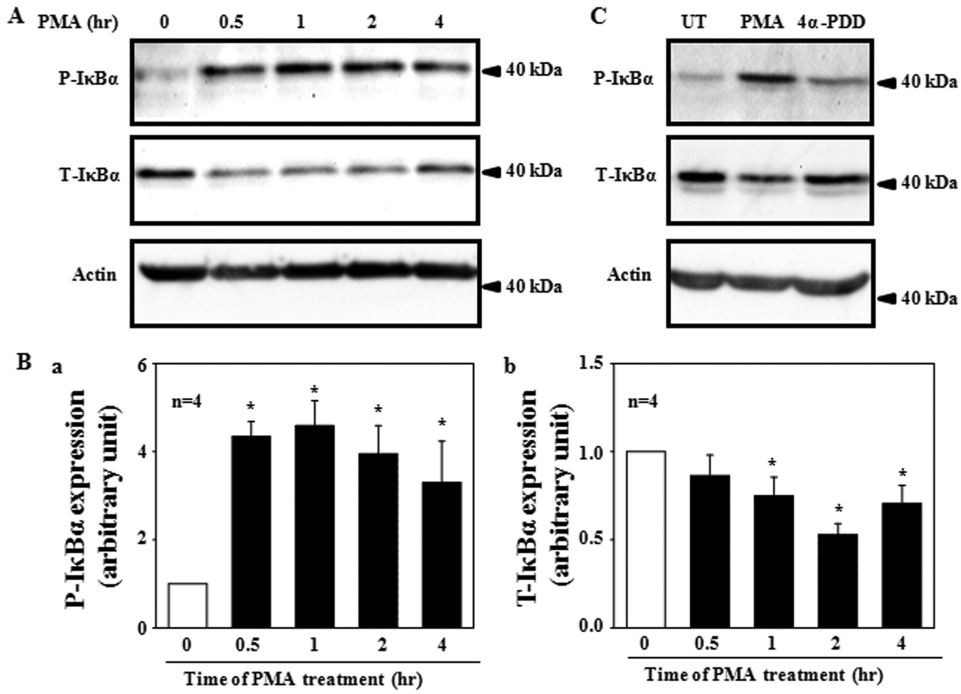

FIGURE 5. **A Western blot shows a time-dependent expression of phosphorylated IκBα (*P-IκBα*) and total IκBα (*T-IκBα*) in human MCs treated with 1 μM PMA in serum-free medium.** *A*, representative experiments are shown. Actin was used as a loading control. *B*, shown are quantifications of P-IκBα (*Ba*) and T-IκBα (*Bb*) by normalization to actin for the experiments indicated in *A*. The value at time 0 was taken as 1. * denotes a significant difference, compared with time 0. *n* indicates the number of independent experiments. *C*, a representative Western blot shows the PMA (1 μM for 0.5 h) and 4α-PDD (1 μM for 0.5 h) effect on P-IκBα and T-IκBα expression in human MCs. Actin was used as a loading control.

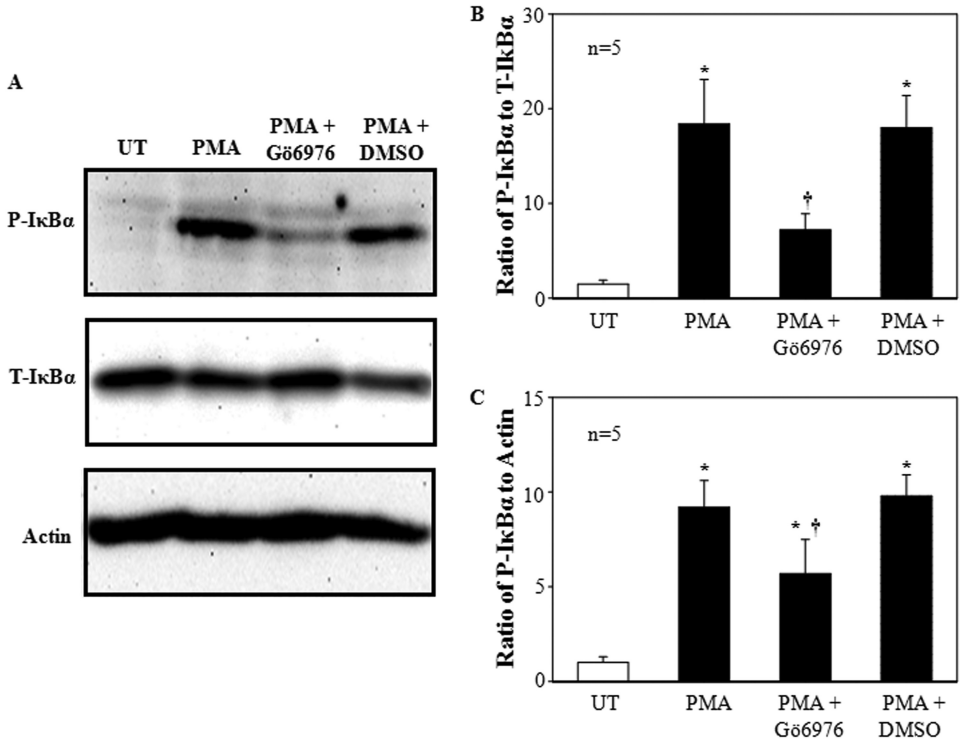

FIGURE 6. **Effect of PKCα and βI inhibition on PMA-induced phosphorylation of IκBα in human MCs.** *A*, a representative Western blot shows the expression levels of P-IκBα and T-IκBα in MCs without treatment (*UT*) and MCs treated with PMA (1 μM for 30 min) with or without pretreatment of Gö6976 (300 nM) or DMSO. Both Gö6976 and DMSO were applied 30 min before PMA treatment. Actin was used as a loading control. *B* and *C*, shown is quantification of P-IκBα expression by normalizing the optical density of P-IκBα bands to that of T-IκBα bands (*B*) or actin (*C*). * denotes $p < 0.05$, *versus* UT; † denotes $p < 0.05$, *versus* both PMA and PMA + DMSO. *n* indicates the number of independent experiments.

known that phosphorylation of, and subsequent degradation of IκBα in response to stimuli is the mechanism for NF-κB activation (39–41). We thus assessed whether the phosphorylation of IκBα occurred in MCs upon PMA treatment. As shown in Fig. 5, PMA treatment (1 μM) resulted in phosphorylation of IκBα. A significant increase occurred within 30 min and was sustained as long as 4 h (Fig. 5, *A* and *Ba*). Furthermore, PMA induced a time-dependent reduction of the total IκBα (Fig. 5, *A* and *Bb*). The PMA effect was specific because 4α-PDD did not evoke phosphorylation and degradation of IκBα (Fig. 5*C*).

Gö6976 Inhibited PMA-induced IκBα Phosphorylation—Our previous study demonstrated that the PKC isoform suppressing TRPC6 expression was PKCα (5). If NF-κB mediated the PKC effect on TRPC6, inhibition of PKCα should depress the PKC-dependent IκBα phosphorylation. As shown in Fig. 6, treatment of MCs with 1 μM PMA for 30 min markedly increased the level of phosphorylated IκBα, whereas pretreatment of the cells with 300 nM Gö6976 (a PKCα and βI inhibitor), but not DMSO (vehicle), significantly prevented IκBα from being phosphorylated (Fig. 6).

PMA Stimulated Nuclear Translocation of NF-κB—After release from its inhibitor IκBα, NF-κB translocates from the cytoplasm to the nucleus for regulation of its target gene transcription (36). Using a Western blot assay on the cell nuclear extracts, we were able to detect a significant increase in the expression levels of p50 and p65, two major subunits of NF-κB in MCs treated with 1 μM PMA. Consistent with IκBα phosphorylation, the nuclear translocation of both p50 and p65 occurred within 30 min after PMA treatment and continued for at least 4 h, the longest time period we observed in this study (Fig. 7, *Aa–c*). However, the total amounts of both p50 and p65 proteins were not altered by the PMA treatments (Fig. 7, *Ba–c*). Immunofluorescence staining also showed the nuclear translocation of NF-κB in response to PMA but not to 4α-PDD (Fig. 7*C*).

PMA Stimulated DNA Binding Activity of NF-κB—To detect if the PKC-stimulated nuclear translocation of NF-κB can be translated to promotion of DNA binding of the transcription factor, EMSA was performed using a commercial probe specific for NF-κB binding (Santa Cruz). Nuclear extracts from unstimulated MCs produced a detectable NF-κB-DNA complex (*lane 2* in Fig. 8*A*). When MCs were treated with PMA (1 μM for 60 min), the formation of the complex was significantly enhanced (*lane 4* in Fig. 8, *A* and *B*), an effect similar to a known NF-κB activator, TNF-α (*lane 8* in Fig. 8*A*). The PMA effect was specific because the same concentration of 4α-PDD did not increase the complex formation (*lane 6* in Fig. 8, *A* and *B*). The formation of the NF-κB-DNA complex was dramatically attenuated by a 50-fold excess of the same unlabeled NF-κB oligonucleotide in the nuclear extracts from all groups of MCs (unstimulated, PMA-treated, 4α-PDD-treated, and TNF-α-treated, corresponding to *lanes 3*, *5*, *7* and *9* in Fig. 8*A*, respectively), indicating that the complex formation was specific.

P65 Was the Predominant NF-κB Subunit Mediating H_2O_2 Effect on TRPC6 Expression—If NF-κB is a mediator for H_2O_2 inhibition on TRPC6 expression, then activation of NF-κB should mimic the H_2O_2 effect. Because TNF-α is a well known NF-κB activator and we have shown that TNF-α promoted

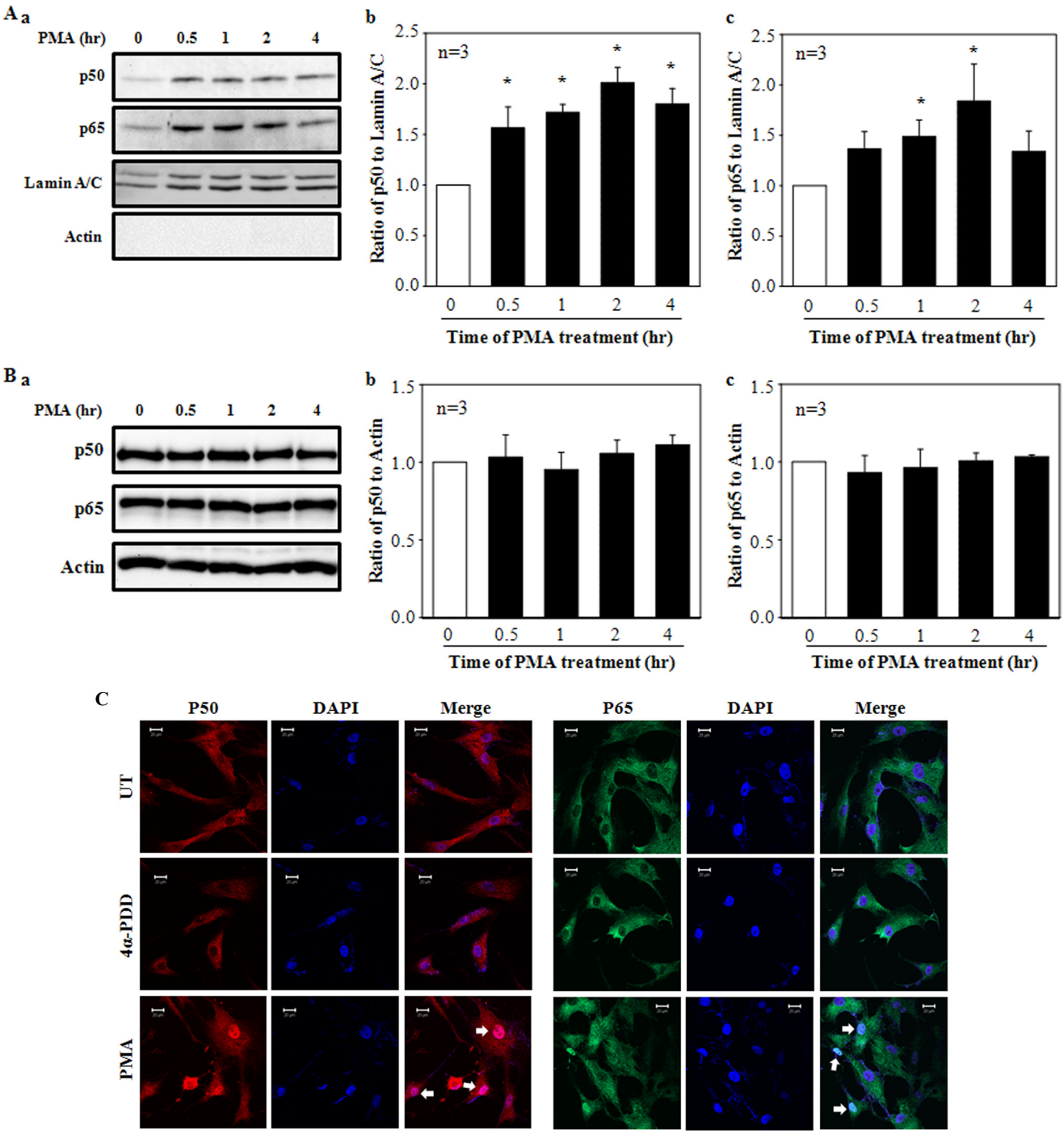

FIGURE 7. **Nuclear translocation of NF-κB in response to PMA treatment in human MCs.** *A* and *B*, a Western blot shows expressions of p50 and p65 NF-κB subunits in the nuclear extracts (*A*) and whole cell lysates (*B*) in MCs with 1 μM PMA treatment for various time periods. *Aa*, shown are representative immunoblots of the nuclear extracts. Lamin A/C was used as a loading control of nuclear proteins. Actin was used to determine whether the nuclear extracts were contaminated by the cytoplasmic fractions. *A*, *b* and *c*, shown is quantification of nuclear p50 and p65 proteins by normalization to lamin A/C from experiments indicated in *Aa*. The value at time 0 of PMA treatment was considered as 1. * denotes $p < 0.05$, *versus* time 0. *n* indicates the number of independent experiments. *Ba*, representative shown are immunoblots of the whole cell lysates. Actin was used as a loading control. *B*, *b* and *c*, shown is quantification of p50 and p65 proteins by normalization to actin from experiments indicated in *Ba*. The value at time 0 of PMA treatment was considered as 1. *n* indicates the number of independent experiments. *C*, shown is immunofluorescence staining of p50 (*red*) and p65 (*green*) in MCs with and without PMA or 4α-PDD at 1 μM for 30 min. *UT* represents MCs without PMA and 4α-PDD treatments. Nuclei were stained with DAPI (*blue*). *Arrows* indicate the nuclear localization of p50 or p65.

NF-κB-DNA binding in MCs (Fig. 8*A*), we then further examined if TNF-α could suppress TRPC6 gene transcription. Similar to H_2O_2, TNF-α (20 ng/ml) evoked a time-dependent inhibition on TRPC6 mRNA expression. The time frames of the effect for both H_2O_2 and TNF-α were the same, and 2 h were required for a significant inhibition (Fig. 9*A*).

To determine if both p50 and p65 or only one of the two subunits were involved in the suppression of TRPC6 transcrip-

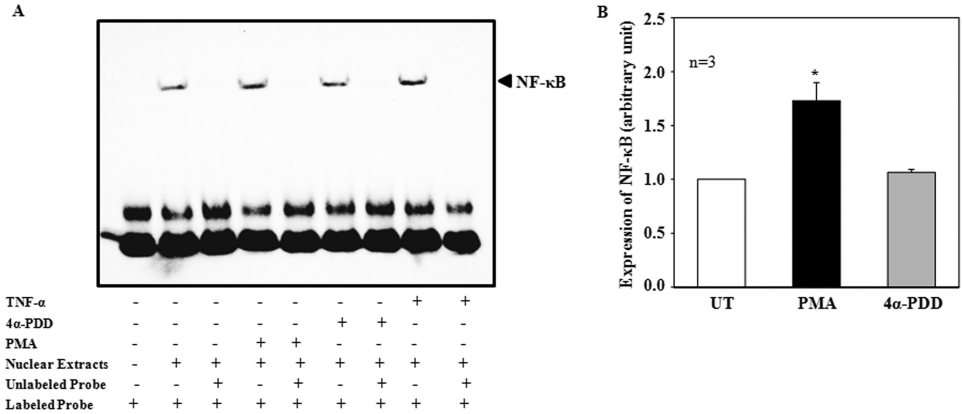

FIGURE 8. **Effect of PKC on DNA-binding activity of NF-κB in human MCs (EMSA).** *A*, the nuclear extracts were extracted from MCs treated with PMA (1 μM for 1 hr) or 4α-PDD (1 μM for 1hr) or TNF-α (20 ng/ml for 1 hr). The unlabeled oligonucleotides were 50 folds greater than the labeled oligonucleotides. *B*, summary data from 3 independent experiments, showing NF-κB expression level by normalizing the NF-κB band in MCs with PMA or 4α-PDD treatment to the band in MCs without treatment (UT). * denotes $p < 0.05$, *versus* UT and 4α-PDD treatment.

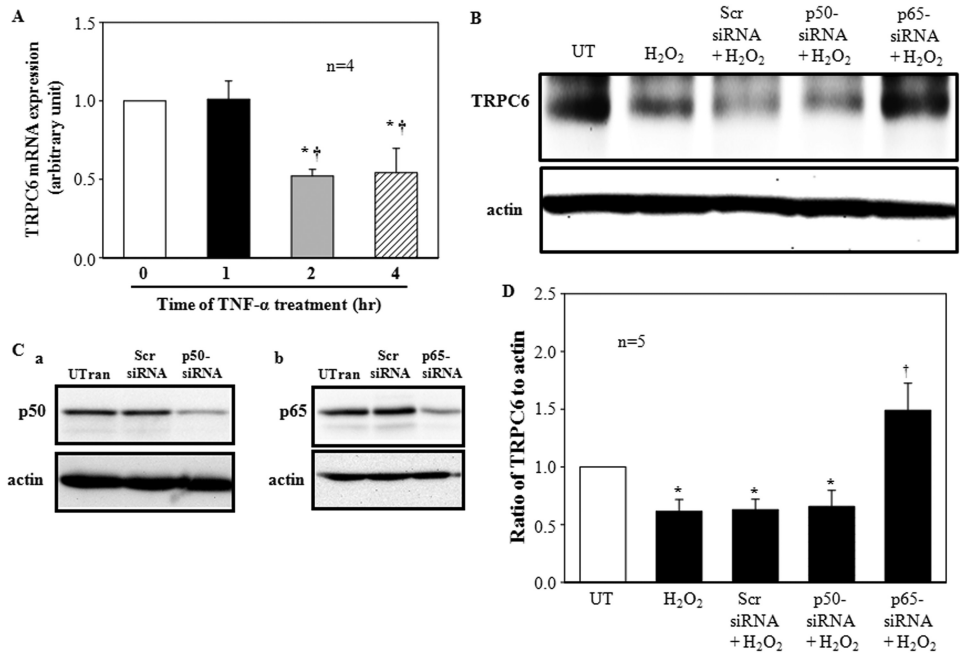

FIGURE 9. **Effect of TNF-α on TRPC6 mRNA expression (*A*) and effect of knockdown of p50 and p65 on H_2O_2-decreased TRPC6 protein expression (*B–D*) in MCs.** *A*, shown is quantitative real time RT-PCR. Cells were without (time 0) or with TNF-α treatment at 20 ng/ml for 1, 2, and 4 h in FBS-free medium. The TRPC6 mRNA level was normalized by β-actin mRNA levels. * denotes $p < 0.05$ compared with time 0, and † denotes $p < 0.05$ compared with 1 h. *n* indicates the number of independent experiments. *B*, shown are representative immunoblots. MCs were either not treated (*UT*) or treated with H_2O_2 (200 μM for 6 h) with or without transfection of siRNA against human p50 (*p50-siRNA*+H_2O_2), p65 (*p65-siRNA*+H_2O_2), or scramble controls (*Scr-siRNA*+H_2O_2). Actin was used as a loading control. *C*, representative immunoblots show p50 (*Ba*) and p65 (*Bb*) expression levels in untransfected MCs (*Utran*) or the MCs transfected with scramble siRNA (*Scr siRNA*) or siRNA against human p50 (*p50-siRNA*) or p65 (*p65-siRNA*). Actin was used as a loading control. *D*, shown are TRPC6 expression levels normalized to actin in all groups shown in *A*, and the value of UT was taken as 1. Data were averaged from four independent experiments. * denotes $p < 0.05$, *versus* both UT and p65-siRNA+H_2O_2, and † denotes $p < 0.05$, *versus* UT. *n* indicates the number of independent experiments.

tion in H2O2/PKC signaling pathway, we individually knocked down the NF-κB subunits using siRNA specifically against human p50 or p65. As shown in Fig. 9, *B* and *C*, H_2O_2 treatment (200 μM for 6 h) significantly reduced the abundance of TRPC6 protein. Knockdown of p65 not only reversed the H_2O_2 effect but also significantly increased the expression level of TRPC6 compared with untransfected cells or scramble siRNA-transfected cells (Fig. 9, *B* and *D*), suggesting that the endogenous p65 might have a tonic effect on TRPC6 transcription. However, knockdown of p50 did not affect the inhibition of H_2O_2 on TRPC6 protein expression (Fig. 9, *B* and *D*). A Western blot showed that the knockdown efficiencies of siRNA p50 and p65 were comparable (Fig. 9*C*). These results suggest that p65 is the subunit mediating the H_2O_2 effect on TRPC6 protein expression in MCs.

PMA Induced p65 Binding to the TRPC6 Promoter in Human MCs—Consistent with a role of p65 in down-regulation of TRPC6 expression in ROS/PKC signaling, ChIP assays showed that PMA stimulated p65, but not a control IgG, binding to the *TRPC6* promoter in human MCs (Fig. 10, *A* and *B*). As a positive control, PMA also stimulated p65 binding to the promoter region of IκBα, a well known target gene of NF-κB (Fig. 10, *A* and *C*). However, PMA did not stimulate p65 binding to a region of genomic DNA between the GAPDH gene and the

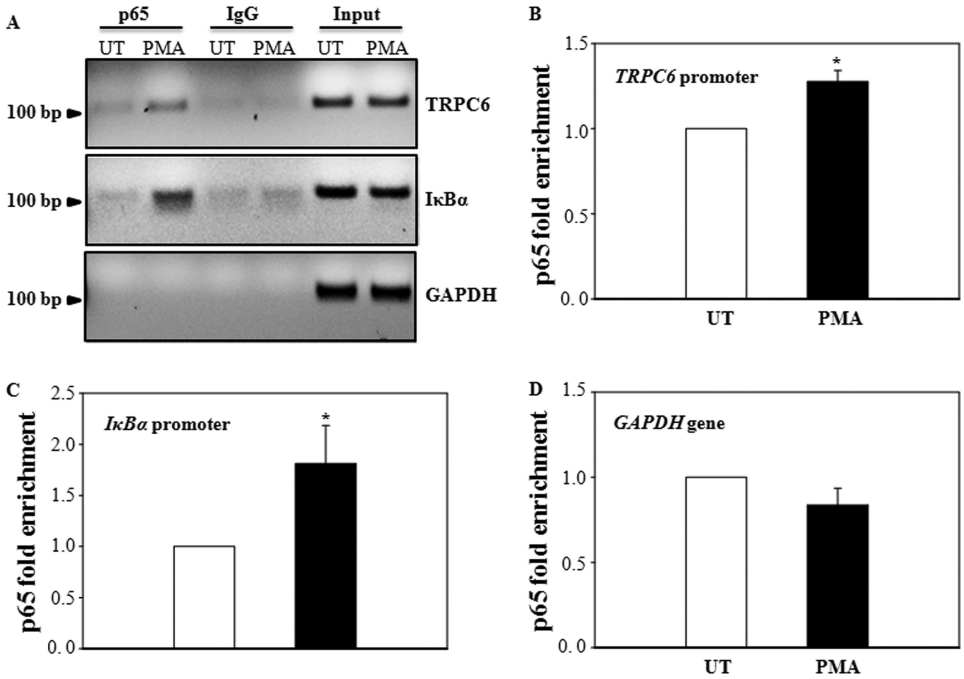

FIGURE 10. **PMA induced p65 binding to the TRPC6 promoter in human MCs.** Cells were with (*PMA*) or without (*UT*) stimulation with 1 μM PMA for 60 min, and ChIP analyses were performed using an anti-p65 antibody. Promoter copy number was quantified by quantitative real-time PCR in duplicate using a specific primer that amplifies an NF-κB binding site in the *TRPC6* or *IκBα* promoter. Normal rabbit IgG was used as a negative control for the specificity of immunoprecipitation. A 174-bp genomic region flanking the *GAPDH* and the chromosome condensation-related SMC-associated protein (*CNAP1*) gene, which does not have an NF-κB binding site, was used as a negative control for the specificity of NF-κB binding to *TRPC6* gene. As a positive control, aliquots (1/10 of immunoprecipitates) of chromatin fragments obtained before immunoprecipitation were also subjected to PCR analysis (*Input*). *A*, a representative experiment shows the NF-κB p65-bound DNA fragments in 2% agarose gel. *B–D*, shown are summary data from four independent experiments presented in *A*. Data are expressed as p65-fold enrichment by normalizing p65-*TRPC6* binding (*B*) or p65-*IκBα* binding (*C*) or p65-*GAPDH* binding (*D*) to their corresponding input chromatins. In *B* and *C*, * denotes $p < 0.05$, compared with UT.

chromosome condensation-related SMC-associated protein (CNAP1) gene, in which there is no transcription factor binding site (Fig. 10, *A* and *D*). These results suggest that the p65-*TRPC6* binding in response to PMA stimulation was specific.

Repression of TRPC6 Transcription by ROS/PKC/p65 Required Histone Deacetylases—Because NF-κB p65 has been reported to recruit histone deacetylase (HDAC) to repress its target gene expression (42, 43), we evaluated the possibility that histone deacetylation was a downstream mechanism for inhibition of *TRPC6* gene transcription in the ROS/PKC/p65 signaling pathway. In agreement with this speculation, co-immunoprecipitation experiments revealed that PMA, but not 4α-PDD, increased associations of NF-κB p65 with HDAC2, a major endogenous HDAC in MCs (44, 45) (Fig. 11*A*). Further ChIP assays were conducted to examine histone H3 acetylation at the *TRPC6* promoter in response to PMA treatment. As shown in Fig. 11*B*, treatment with PMA, but not 4α-PDD, resulted in a strong decrease in histone acetylation at the *TRPC6* promoter. Furthermore, specific knockdown of HDAC2 by siRNA significantly prevented a H_2O_2-induced decrease in TRPC6 mRNA expression (Figs. 1 and 11*C*). Consistently, pretreatment of MCs with HDAC inhibitor, trichostatin A (*TSA*) reversed H_2O_2-induced decrease in TRPC6 protein expression (Fig. 11, *D* and *E*). These results suggest that HDACs mediated the repressive effect of ROS/PKC/NF-κB p65 on TRPC6.

DISCUSSION

Although acute regulation of TRPC6 channel has been well documented (3, 11, 13, 15–19, 46, 47), a long term controlling mechanism, particularly at a transcriptional level, remains unknown to a large extent. We have previously described a ROS/PKC pathway for negative regulation of TRPC6 protein expression in kidney MCs (5). The present study provided evidence that NF-κB is a key molecule downstream of ROS/PKC in the cascade of *TRPC6* gene regulation in kidney cells. The evidence includes the following: 1) NF-κB inhibition significantly attenuated H_2O_2 and/or PKC activation-induced decrease in TRPC6 protein expression, 2) NF-κB activation could mimic the H_2O_2/PKC effect on TRPC6 expression, 3) PKC could activate NF-κB, stimulate its nuclear translocation, and further its binding to the *TRPC6* promoter, and finally 4) activation and inhibition of NF-κB significantly suppressed and enhanced TRPC6-mediated Ca^{2+} entry, respectively. NF-κB is a transcription factor that participates in a wide range of cellular responses, such as inflammation and proliferation when a cell is insulted by pathogenic stimuli (43, 48, 49). Like NF-κB, TRPC6 is also involved in inflammatory responses (50, 51), and TRPC6-associated Ca^{2+} entry is also associated with cell proliferation (2, 52, 53). Thus, the repression of *TRPC6* gene by NF-κB could provide a protective mechanism or brake mechanism to prevent the occurrence of vicious reaction chains when the cells are continuously exposed to noxious stimuli like oxidative stress observed in many diseases.

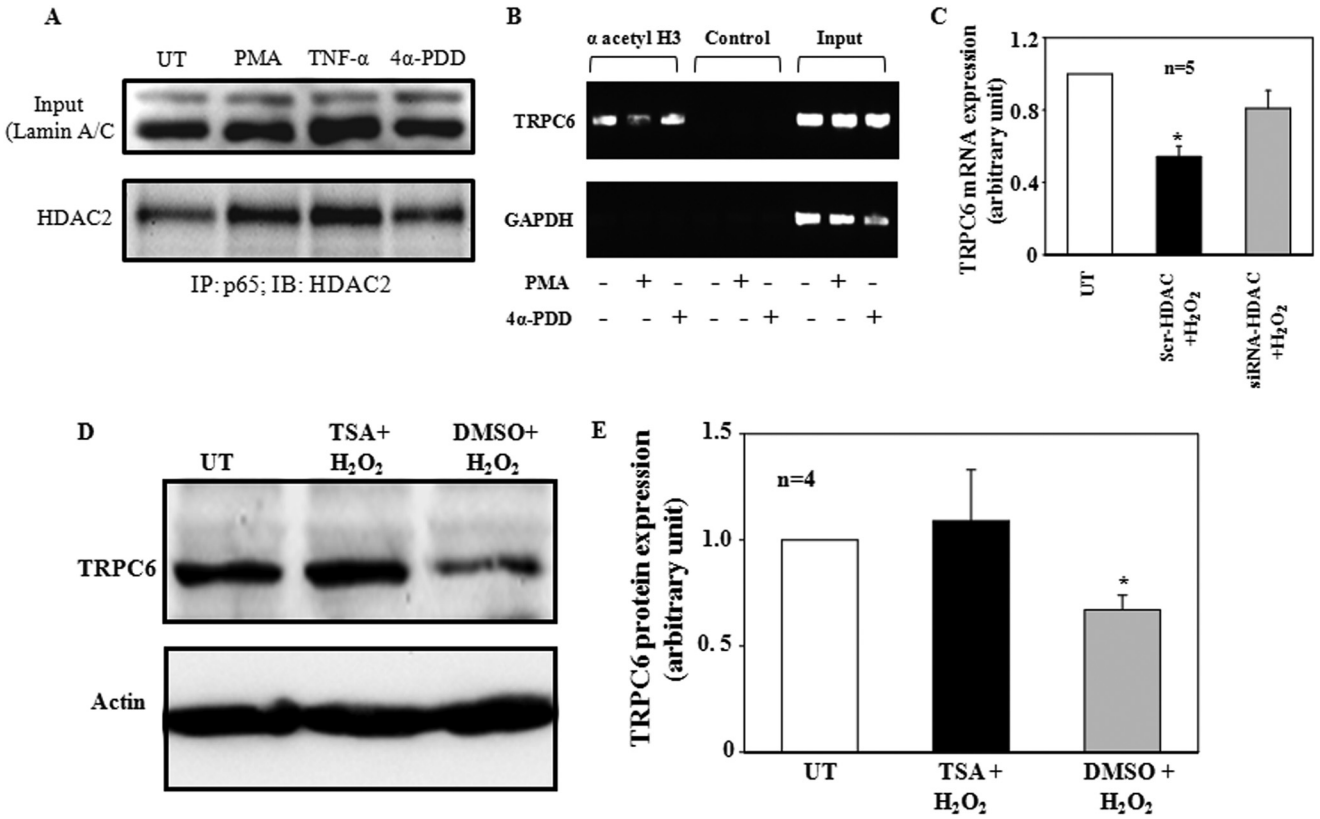

FIGURE 11. *A*, a coimmunoprecipitation assay shows an increase in association of nuclear p65 with HDAC by activation of PKC. Human MCs were stimulated with 1 μM PMA or 4α-PDD or 20 ng/ml TNF-α for 1 h. Nuclear extracts (50 μg) were immunoprecipitated (*IP*) with 2 μg of p65 antibody and immunoblotted (*IB*) with HDAC antibody. Lamin A/C from 10 μg of the nuclear extracts was used as input. TNF-α and 4α-PDD were used as a positive and a negative control for PMA, respectively. The image was representative from three independent experiments. *B*, ChIP assays, showing PMA but not 4α-PDD stimulation, induced histone H3 deacetylation at the *TRPC6* promoter. Human MCs were without stimulation (*UT*) or were stimulated with 1 μM PMA or 4α-PDD for 1 h, and ChIP assays were performed using an antibody directed to acetylated histone H3 (lysines 9 and 14). The presence of acetylated histone H3 was detected by PCR. Normal rabbit IgG was used as a negative control for the specificity of the antibody. *GAPDH* and input were described in Fig. 10. The images were representative ones from three separate experiments. *C*, quantitative real time RT-PCR shows the effect of knockdown of HDAC2 by siRNA on H2O2-induced decrease in TRPC6 mRNA in human MCs. *UT*, MCs without transfection and without H_2O_2 treatment. * denotes $p < 0.05$ *versus* both UT and siRNA-HDAC group. *n* indicates the number of independent experiments. *D*, representative immunoblots show TRPC6 protein expressions in MCs without H_2O_2 treatment (*UT*) or treated with H_2O_2 (200 μM for 6 h) with or without prior incubation with trichostatin A (*TSA*, 3.3 μM for 24 h) or DMSO (vehicle control). Actin was used as a loading control. *E*, shown are summary data from the experiments presented in *D*. TRPC6 protein expression levels were normalized to actin. * denotes $p < 0.05$, *versus* both UT and trichostatin A $+H_2O_2$. *n* indicates the number of independent experiments.

An earlier study by Yu *et al.* (6) reported that NF-κB promoted *TRPC6* gene transcription in pulmonary artery smooth muscle cells from idiopathic pulmonary arterial hypertension patients harboring the −254C→G single-nucleotide polymorphism. This single nucleotide mutation in *TRPC6* gene promoter creates an additional NF-κB binding site that confers the stimulatory effect of NF-κB. The opposite effect of NF-κB observed in the present study suggests that the native and mutation-generated NF-κB binding consensuses may function differently in regulation of *TRPC6* promoter activity. Indeed, in addition to multiple NF-κB binding sites, the binding sites for many other transcription factors are also present in the promoter region of *TRPC6*. It is possible that the particular −254G-generated new NF-κB binding site in idiopathic pulmonary arterial hypertension patients may facilitate interactions of various transcription factors (*e.g.* NFAT, AP-1) to promote *TRPC6* gene transcription (54). This is supported by the data from the same study of Yu *et al.* (6) in which TRPC6 expression was not significantly altered by NF-κB activation in the pulmonary artery smooth muscle cells without the additional binding site. Another possibility for the difference between Yu *et al.* (6) and our studies might be simply due to a cell type-specific effect of NF-κB. For instance, NF-κB represses anti-apoptotic gene expression in U-2 OS human osteosarcoma cells (55) but stimulates anti-apoptotic genes in HeLa human carcinoma cells (56) in response to the chemotherapeutic drugs (daunorubicin/doxorubicin). Although the mechanism for the cell type-specific effect is not clear, the nature of co-factors that are required for NF-κB function in different types of cells might play a role. It is possible that in kidney MCs, repressive co-factors are predominant, whereas in the pulmonary artery smooth muscle cells, a strong interaction between NF-κB and its co-activators may play a major role.

NF-κB stimulates or represses target gene transcription differently depending on the nature of the bound NF-κB homo- or heterodimer (36). In general, heterodimers of p65/p50 are transcriptional activators, whereas the homodimers of p50/p50 act as transcriptional repressors (57–59). In the present study, knockdown of p65, but not p50, prevented a H_2O_2-induced TRPC6 decrease (Fig. 9, *B* and *D*). We thereby infer that although ROS/PKC stimulates the nuclear translocation of both p50 and p65 subunits in MCs, it is a p65 subunit that

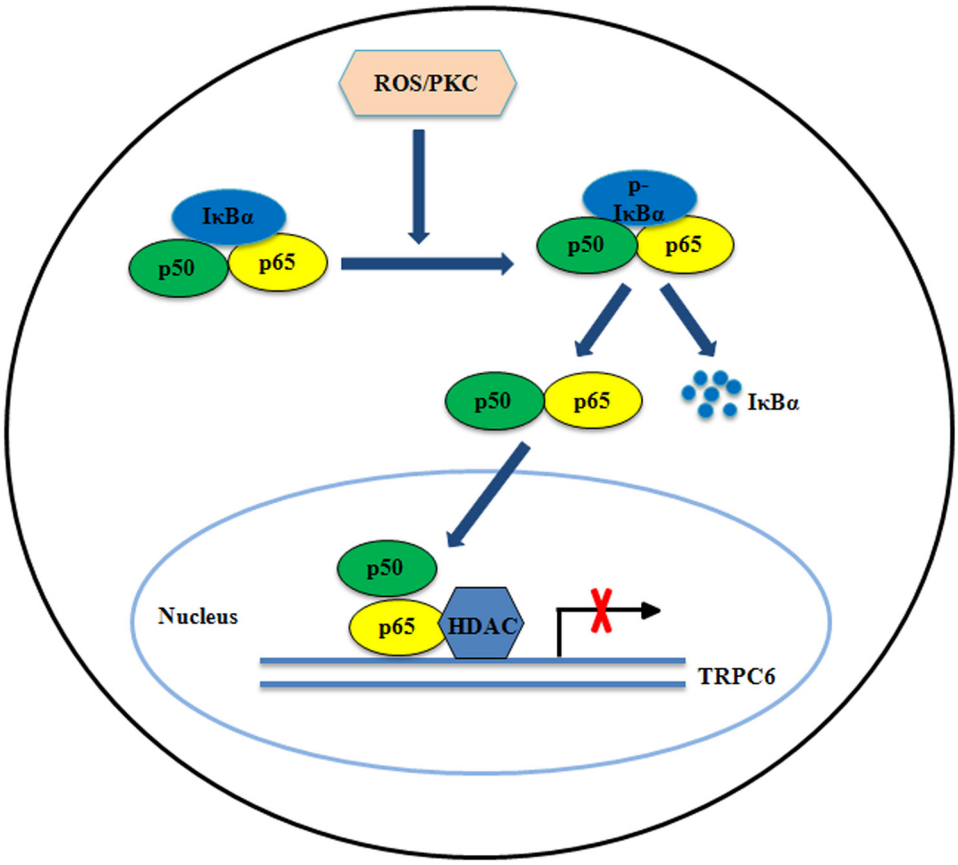

FIGURE 12. **Schematic illustration of the down-regulation of *TRPC6* expression by ROS/PKC signaling in human MCs.** In MCs, activation of PKC by ROS causes phosphorylation and degradation of IκBα in the cytoplasm. The NF-κB (p50 and p65 subunits) freed from the inhibitory IκBα translocates to the nucleus. In the nucleus, p65 subunit binds to the NF-κB binding site within the *TRPC6* promoter and recruits HDACs to repress the gene transcription.

represses *TRPC6* gene transcription. Although most known actions of NF-κB p65 subunit involve induction of gene transcription, it may also actively repress gene expression (42, 43, 55, 60). Several mechanisms are involved in the p65-dependent gene repression. Recently, the importance of HDAC activity has become apparent. Histone deacetylation mediated by HDAC generally leads to transcriptional repression. NF-κB, primarily the p65 subunit, can bind HDAC, recruit the enzymes to its target gene, and consequently change p65 activity from induction to repression of transcription (42, 43, 60, 61). For instance, HDAC activity is required for p65-dependent repression of the peroxisome proliferator-activated receptor δ target gene in human keratinocytes (61), of the Klotho gene in mouse kidney cells (43), and of anti-apoptotic genes in human osteosarcoma cells (55). The present study suggests that histone deacetylation may also be a mechanism for the p65-mediated *TRPC6* gene repression in MCs because 1) activation of PKC increased associations of p65 with HDAC and decreased histone acetylation at the TRPC6 promoter (Fig. 11, *A* and *B*), and 2) biological and pharmacological inhibition of HDAC prevented a H_2O_2-induced decrease in TRPC6 mRNA and protein expressions, respectively (Fig. 11, *C–E*). HDACs are expressed in MCs and regulate MC function by regulating transcription of several genes (62–64). Because TRPC6 participates in MC contractile function, and dysfunction of TRPC6 channels may contribute to diabetic hyperfiltration (5), our findings on the HDACs-controlled *TRPC6* expression may provide a means of treating glomerular diseases at gene transcriptional level.

In addition to NF-κB, other transcription factors may also act on the *TRPC6* gene as either an activator or a repressor. By searching transcription factor consensus sequences in *TRPC6* promoter region, we found multiple potential binding sites for a variety of candidate transcription factors within up to −2000 nucleotides from *TRPC6* transcription start site, including AP-1 and SP-1. It is possible that some of these factors may also regulate the TRPC6 gene through a mechanism independent of NF-κB. Alternatively, one or more the transcription factors (activators) interact with NF-κB in the *TRPC6* promoter region and consequently lose their capability of gene transactivation. Indeed, antagonistic and synergistic interactions between NF-κB and other promoter-bound transcription factors have been previously described. For instance, in lung epithelial cells p65 interacts with SP1, a potent transcription activator, to produce transcription repression of the *Bmp4* gene (65). Whether the similar mechanism also exists in MCs needs further investigation.

In summary, the present study provides a molecular mechanism for ROS/PKC-regulated TRPC6 channels at the gene transcriptional level. The diagram in Fig. 12 schematically describes a contribution of NF-κB to this regulatory pathway. Given that the maintenance of cell homeostasis is life-span work and development of many diseases is a long and progres-

sive course, understanding the mechanisms for chronic regulation of TRPC6 channel has important physiological and pathological significance.

REFERENCES

1. Clapham, D. E. (2003) TRP channels as cellular sensors. *Nature* **426,** 517–524
2. Abramowitz, J., and Birnbaumer, L. (2009) Physiology and pathophysiology of canonical transient receptor potential channels. *FASEB J.* **23,** 297–328
3. Ding, Y., Winters, A., Ding, M., Graham, S., Akopova, I., Muallem, S., Wang, Y., Hong, J. H., Gryczynski, Z., Yang, S. H., Birnbaumer, L., and Ma, R. (2011) Reactive oxygen species-mediated TRPC6 activation in vascular myocytes, a mechanism for vasoconstrictor-regulated vascular tone. *J. Biol. Chem.* **286,** 31799–31809
4. Graham, S., Ding, M., Sours-Brothers, S., Yorio, T., Ma, J. X., and Ma, R. (2007) Down-regulation of TRPC6 protein expression by high glucose, a possible mechanism for the impaired Ca^{2+} signaling in glomerular mesangial cells. *Am. J. Physiol. Renal Physiol.* **293,** F1381–F1390
5. Graham, S., Gorin, Y., Abboud, H. E., Ding, M., Lee, D. Y., Shi, H., Ding, Y., and Ma, R. (2011) Abundance of TRPC6 protein in glomerular mesangial cells is decreased by ROS and PKC in diabetes. *Am. J. Physiol. Cell Physiol.* **301,** C304–C315
6. Yu, Y., Keller, S. H., Remillard, C. V., Safrina, O., Nicholson, A., Zhang, S. L., Jiang, W., Vangala, N., Landsberg, J. W., Wang, J. Y., Thistlethwaite, P. A., Channick, R. N., Robbins, I. M., Loyd, J. E., Ghofrani, H. A., Grimminger, F., Schermuly, R. T., Cahalan, M. D., Rubin, L. J., and Yuan, J. X. (2009) A functional single-nucleotide polymorphism in the *TRPC6* gene promoter associated with idiopathic pulmonary arterial hypertension. *Circulation* **119,** 2313–2322
7. Yu, Y., Fantozzi, I., Remillard, C. V., Landsberg, J. W., Kunichika, N., Platoshyn, O., Tigno, D. D., Thistlethwaite, P. A., Rubin, L. J., and Yuan, J. X. (2004) Enhanced expression of transient receptor potential channels in idiopathic pulmonary arterial hypertension. *Proc. Natl. Acad. Sci. U.S.A.* **101,** 13861–13866
8. Winn, M. P., Conlon, P. J., Lynn, K. L., Farrington, M. K., Creazzo, T., Hawkins, A. F., Daskalakis, N., Kwan, S. Y., Ebersviller, S., Burchette, J. L., Pericak-Vance, M. A., Howell, D. N., Vance, J. M., and Rosenberg, P. B. (2005) A mutation in the TRPC6 cation channel causes familial focal segmental glomerulosclerosis. *Science* **308,** 1801–1804
9. Winn, M. P., Daskalakis, N., Spurney, R. F., and Middleton, J. P. (2006) Unexpected role of TRPC6 channel in familial nephrotic syndrome. Does it have clinical implications? *J. Am. Soc. Nephrol.* **17,** 378–387
10. Onohara, N., Nishida, M., Inoue, R., Kobayashi, H., Sumimoto, H., Sato, Y., Mori, Y., Nagao, T., and Kurose, H. (2006) TRPC3 and TRPC6 are essential for angiotensin II-induced cardiac hypertrophy. *EMBO J.* **25,** 5305–5316
11. Estacion, M., Li, S., Sinkins, W. G., Gosling, M., Bahra, P., Poll, C., Westwick, J., and Schilling, W. P. (2004) Activation of human TRPC6 channels by receptor stimulation. *J. Biol. Chem.* **279,** 22047–22056
12. Mizuno, N. (1999) Molecular cloning and characterization of rat *trp* homologues from brain. *Brain Res. Mol. Brain Res.* **64,** 41–51
13. Hofmann, T., Obukhov, A. G., Schaefer, M., Harteneck, C., Gudermann, T., and Schultz, G. (1999) Direct activation of human TRPC6 and TRPC3 channels by diacylglycerol. *Nature* **397,** 259–263
14. Graham, S., Ding, M., Ding, Y., Sours-Brothers, S., Luchowski, R., Gryczynski, Z., Yorio, T., Ma, H., and Ma, R. (2010) Canonical transient receptor potential 6 (TRPC6), a redox-regulated cation channel. *J. Biol. Chem.* **285,** 23466–23476
15. Weissmann, N., Sydykov, A., Kalwa, H., Storch, U., Fuchs, B., Mederos y Schnitzler, M., Brandes, R. P., Grimminger, F., Meissner, M., Freichel, M., Offermanns, S., Veit, F., Pak, O., Krause, K. H., Schermuly, R. T., Brewer, A. C., Schmidt, H. H., Seeger, W., Shah, A. M., Gudermann, T., Ghofrani, H. A., and Dietrich, A. (2012) Activation of TRPC6 channels is essential for lung ischaemia-reperfusion induced oedema in mice. *Nat. Commun.* **3,** 649
16. Shen, B., Kwan, H. Y., Ma, X., Wong, C. O., Du, J., Huang, Y., and Yao, X. (2011) cAMP activates TRPC6 channels via the phosphatidylinositol 3-kinase (PI3K)-protein kinase B (PKB)-mitogen-activated protein kinase (MEK)-ERK1/2 signaling pathway. *J. Biol. Chem.* **286,** 19439–19445
17. Monet, M., Francoeur, N., and Boulay, G. (2012) Involvement of phosphoinositide 3-kinase and PTEN in the mechanism of activation of TRPC6 in vascular smooth muscle cells. *J. Biol. Chem.* **287,** 17672–17681
18. Bousquet, S. M., Monet, M., and Boulay, G. (2010) Protein kinase C-dependent phosphorylation of transient receptor potential canonical 6 (TRPC6) on serine 448 causes channel inhibition. *J. Biol. Chem.* **285,** 40534–40543
19. Cayouette, S., Lussier, M. P., Mathieu, E. L., Bousquet, S. M., and Boulay, G. (2004) Exocytotic insertion of TRPC6 channel into the plasma membrane upon G_q protein-coupled receptor activation. *J. Biol. Chem.* **279,** 7241–7246
20. Shah, S. V., Baliga, R., Rajapurkar, M., and Fonseca, V. A. (2007) Oxidants in chronic kidney disease. *J. Am. Soc. Nephrol.* **18,** 16–28
21. Hayden, M. R., and Sowers, J. R. (2007) Redox imbalance in diabetes. *Antioxid. Redox. Signal.* **9,** 865–867
22. Banday, A. A., Fazili, F. R., and Lokhandwala, M. F. (2007) Oxidative stress causes renal dopamine D1 receptor dysfunction and hypertension via mechanisms that involve nuclear factor-*k*B and protein kinase C. *J. Am. Soc. Nephrol.* **18,** 1446–1457
23. Nicolls, M. R., Haskins, K., and Flores, S. C. (2007) Oxidant stress, immune dysregulation, and vascular function in type 1 diabetes. *Antioxid. Redox. Signal.* **9,** 879–889
24. Abboud, H. E. (2012) Mesangial cell biology. *Exp. Cell Res.* **318,** 979–985
25. Stockand, J. D., and Sansom, S. C. (1998) Glomerular mesangial cells. Electrophysiology and regulation of contraction. *Physiol. Rev.* **78,** 723–744
26. Schlöndorff, D., and Banas, B. (2009) The mesangial cell revisited. No cell is an island. *J. Am. Soc. Nephrol.* **20,** 1179–1187
27. Kashgarian, M., and Sterzel, R. B. (1992) The pathobiology of the mesangium. *Kidney Int.* **41,** 524–529
28. Kanwar, Y. S., Akagi, S., Sun, L., Nayak, B., Xie, P., Wada, J., Chugh, S. S., and Danesh, F. R. (2005) Cell biology of diabetic kidney disease. *Nephron. Exp. Nephrol.* **101,** e100-e110
29. Scindia, Y. M., Deshmukh, U. S., and Bagavant, H. (2010) Mesangial pathology in glomerular disease. Targets for therapeutic intervention. *Adv. Drug Deliv. Rev.* **62,** 1337–1343
30. Sours, S., Du, J., Chu, S., Ding, M., Zhou, X. J., and Ma, R. (2006) Expression of canonical transient receptor potential (TRPC) proteins in human glomerular mesangial cells. *Am. J. Physiol. Renal Physiol.* **290,** F1507–F1515
31. Sours-brothers, S., Ding, M., Graham, S., and Ma, R. (2009) Interaction between TRPC1/TRPC4 assembly and STIM1 contributes to store-operated Ca^{2+} entry in mesangial cells. *Exp. Biol. Med.* **234,** 673–682
32. Canty, T. G., Boyle, E. M., Farr, A., Morgan, E. N., Verrier, E. D., and Pohlman, T. H. (1999) Oxidative stress induces NF-κB nuclear translocation without degradation of IκBα. *Circulation* **100,** Suppl. II, 361–364
33. Shi, X. Z., Lindholm, P. F., and Sarna, S. K. (2003) NF-κB activation by oxidative stress and inflammation suppresses contractility in colonic circular smooth muscle cells. *Gastroenterology* **124,** 1369–1380
34. Tsai, K. L., Chiu, T. H., Tsai, M. H., Chen, H. Y., and Ou, H. C. (2012) Vinorelbine-induced oxidative injury in human endothelial cells mediated by AMPK/PKC/NADPH/NF-κB pathways. *Cell Biochem. Biophys.* **62,** 467–479
35. Chuang, H. C., Lan, J. L., Chen, D. Y., Yang, C. Y., Chen, Y. M., Li, J. P., Huang, C. Y., Liu, P. E., Wang, X., and Tan, T. H. (2011) The kinase GLK controls autoimmunity and NF-κB signaling by activating the kinase PKC-θ in T cells. *Nat. Immunol.* **12,** 1113–1118
36. Nishikori, M. (2005) Classical and alternative NF-κB activation pathways and their roles in lymphoid malignancies. *J. Clin. Exp. Hematopathol.* **45,** 15–24
37. Müller, M., Essin, K., Hill, K., Beschmann, H., Rubant, S., Schempp, C. M., Gollasch, M., Boehncke, W. H., Harteneck, C., Müller, W. E., and Leuner, K. (2008) Specific TRPC6 channel activation, a novel approach to stimulate keratinocyte differentiation. *J. Biol. Chem.* **283,** 33942–33954
38. Leuner, K., Kazanski, V., Müller, M., Essin, K., Henke, B., Gollasch, M., Harteneck, C., and Müller, W. E. (2007) Hyperforin. A key constituent of

St. John's wort specifically activates TRPC6 channels. *FASEB J.* **21,** 4101–4111
39. Kretz-Remy, C., Mehlen, P., Mirault, M. E., and Arrigo, A. P. (1996) Inhibition of IκB-α phosphorylation and degradation and subsequent NF-κB activation by glutathione peroxidase overexpression. *J. Cell Biol.* **133,** 1083–1093
40. Beg, A. A., Finco, T. S., Nantermet, P. V., and Baldwin, A. (1993) Tumor necrosis factor and interleukin-1 lead to phosphorylation and loss of IκBα. A mechanism for NF-κB activation. *Mol. Cell. Biol.* **13,** 3301–3310
41. Ghosh, S., and Baltimore, D. (1990) Activation *in vitro* of NF-κB by phosphorylation of its inhibitor IκB. *Nature* **344,** 678–682
42. Hong, C. Y., Park, J. H., Seo, K. H., Kim, J. M., Im, S. Y., Lee, J. W., Choi, H. S., and Lee, K. (2003) Expression of *MIS* in the testis is down-regulated by tumor necrosis factor α through the negative regulation of SF-1 transactivation by NF-κB. *Mol. Cell. Biol.* **23,** 6000–6012
43. Moreno, J. A., Izquierdo, M. C., Sanchez-Niño, M. D., Suárez-Alvarez, B., Lopez-Larrea, C., Jakubowski, A., Blanco, J., Ramirez, R., Selgas, R., Ruiz-Ortega, M., Egido, J., Ortiz, A., and Sanz, A. B. (2011) The inflammatory cytokines TWEAK and TNFα reduce renal klotho expression through NFκB. *J. Am. Soc. Nephrol.* **22,** 1315–1325
44. Yu, Z., Zhang, W., and Kone, B. C. (2002) Histone Deacetylases augment cytokine induction of the iNOS gene. *J. Am. Soc. Nephrol.* **13,** 2009–2017
45. Noh, H., Oh, E. Y., Seo, J. Y., Yu, M. R., Kim, Y. O., Ha, H., and Lee, H. B. (2009) Histone deacetylase-2 is a key regulator of diabetes and transforming growth factor-β1-induced renal injury. *Am. J. Physiol. Renal Physiol.* **297,** F729–F739
46. Reiser, J., Polu, K. R., Möller, C. C., Kenlan, P., Altintas, M. M., Wei, C., Faul, C., Herbert, S., Villegas, I., Avila-Casado, C., McGee, M., Sugimoto, H., Brown, D., Kalluri, R., Mundel, P., Smith, P. L., Clapham, D. E., and Pollak, M. R. (2005) TRPC6 is a glomerular slit diaphragm-associated channel required for normal renal function. *Nat. Genet.* **37,** 739–744
47. Inoue, R., Jensen, L. J., Jian, Z., Shi, J., Hai, L., Lurie, A. I., Henriksen, F. H., Salomonsson, M., Morita, H., Kawarabayashi, Y., Mori, M., Mori, Y., and Ito, Y. (2009) Synergistic activation of vascular TRPC6 channel by receptor and mechanical stimulation via phospholipase C/diacylglycerol and phospholipase A_2/ω-hydroxylase/20-HETE pathways. *Circ. Res.* **104,** 1399–1409
48. Kim, J. M., Cho, H. H., Lee, S. Y., Hong, C. P., Yang, J. w., Kim, Y. S., Suh, K. T., and Jung, J. S. (2012) Role of IRAK1 on TNF-induced proliferation and NF-κB activation in human bone marrow mesenchymal stem cells. *Cell Physiol. Biochem.* **30,** 49–60
49. Gastonguay, A., Berg, T., Hauser, A. D., Schuld, N., Lorimer, E., and Williams, C. L. (2012) The role of Rac1 in the regulation of NF-κB activity, cell proliferation, and cell migration in non-small cell lung carcinoma. *Cancer Biol. Ther.* **13,** 647–656
50. Hamid, R., and Newman, J. H. (2009) Evidence for inflammatory signaling in idiopathic pulmonary artery hypertension. TRPC6 and nuclear factor-κB. *Circulation* **119,** 2297–2298
51. Sel, S., Rost, B. R., Yildirim, A. O., Sel, B., Kalwa, H., Fehrenbach, H., Renz, H., Gudermann, T., and Dietrich, A. (2008) Loss of classical transient receptor potential 6 channel reduces allergic airway response. *Clin. Exp. Allergy* **38,** 1548–1558
52. Yu, Y., Sweeney, M., Zhang, S., Platoshyn, O., Landsberg, J., Rothman, A., and Yuan, J. X. (2003) PDGF stimulates pulmonary vascular smooth muscle cell proliferation by up-regulating TRPC6 expression. *Am. J. Physiol. Cell Physiol.* **284,** C316–C330
53. Ge, R., Tai, Y., Sun, Y., Zhou, K., Yang, S., Cheng, T., Zou, Q., Shen, F., and Wang, Y. (2009) role of TRPC6 channels in VEGF-mediated angiogenesis. *Cancer Lett.* **283,** 43–51
54. Kuwahara, K., Wang, Y., McAnally, J., Richardson, J. A., Bassel-Duby, R., Hill, J. A., and Olson, E. N. (2006) TRPC6 fulfills a calcineurin signaling circuit during pathologic cardiac remodeling. *J. Clin. Invest.* **116,** 3114–3126
55. Campbell, K. J., Rocha, S., and Perkins, N. D. (2004) Active repression of antiapoptotic gene expression by RelA(p65) NF-κB. *Mol. Cell* **13,** 853–865
56. Bottero, V., Busuttil, V., Loubat, A., Magné, N., Fischel, J. L., Milano, G., and Peyron, J. F. (2001) Activation of nuclear factor κB through the IKK complex by the topoisomerase poisons SN38 and doxorubicin. A brake to apoptosis in HeLa human carcinoma cells. *Cancer Res.* **61,** 7785–7791
57. Satou, R., Miyata, K., Katsurada, A., Navar, L. G., and Kobori, H. (2010) Tumor necrosis factor-α suppresses angiotensinogen expression through formation of a p50/p50 homodimer in human renal proximal tubular cells. *Am. J. Physiol. Cell Physiol.* **299,** C750–C759
58. Hirano, F., Tanaka, H., Hirano, Y., Hiramoto, M., Handa, H., Makino, I., and Scheidereit, C. (1998) Functional interference of Sp1 and NF-κB through the same DNA binding site. *Mol. Cell. Biol.* **18,** 1266–1274
59. Höcherl, K., Schmidt, C., Kurt, B., and Bucher, M. (2010) Inhibition of NF-κB ameliorates sepsis-induced down-regulation of aquaporin-2/V_2 receptor expression and acute renal failure *in vivo*. *Am. J. Physiol. Renal Physiol.* **298,** F196–F204
60. Lu, X., Farmer, P., Rubin, J., and Nanes, M. S. (2004) Integration of the NFκB p65 subunit into the vitamine D receptor transcriptional complex. Identification of p65 domains that inhibit 1,25-dihydroxyvitamine D3-stimulated transcription. *J. Cell Biochem.* **92,** 833–848
61. Aarenstrup, L., Flindt, E. N., Otkjaer, K., Kirkegaard, M., Andersen, J. S., and Kristiansen, K. (2008) HDAC activity is required for p65/Rel-dependent repression of PPARγ-mediated transactivation in human keratinocytes. *J. Invest. Dermatol.* **128,** 1095–1106
62. Freidkin, I., Herman, M., Tobar, A., Chagnac, A., Ori, Y., Korzets, A., and Gafter, U. (2010) Effects of histone deacetylase inhibitors on rat mesangial cells. *Am. J. Physiol. Renal Physiol.* **298,** F426–F434
63. Kume, S., Haneda, M., Kanasaki, K., Sugimoto, T., Araki, S., Isshiki, K., Isono, M., Uzu, T., Guarente, L., Kashiwagi, A., and Koya, D. (2007) SIRT1 inhibits transforming growth factor β-induced apoptosis in glomerular mesangial cells via Smad7 deacetylation. *J. Biol. Chem.* **282,** 151–158
64. Yu, Z., and Kone, B. C. (2006) Targeted histone H4 acetylation via phosphoinositide 3-kinase- and p70s6-kinase-dependent pathways inhibits iNOS induction in mesangial cells. *Am. J. Physiol. Renal Physiol.* **290,** F496–F502
65. Zhu, N. L., Li, C., Huang, H. H., Sebald, M., Londhe, V. A., Heisterkamp, N., Warburton, D., Bellusci, S., and Minoo, P. (2007) TNF-α represses transcription of human bone morphogenetic protein-4 in lung epithelial cells. *Gene* **393,** 70–80